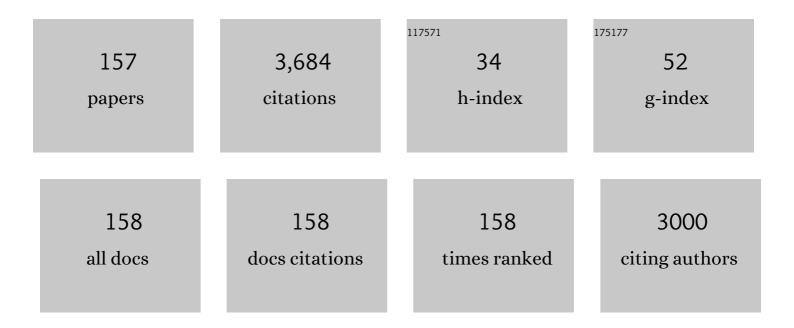
R D K Misra

List of Publications by Year in descending order

Source: https://exaly.com/author-pdf/654789/publications.pdf Version: 2024-02-01



#	Article	IF	CITATIONS
1	Biocompatibility and adhesion response of magnesium-hydroxyapatite/strontium-titania (Mg-HAp/) Tj ETQq1 1 0	.784314 t 1.5	rgBT/Overloo
2	Effects of ECAP extrusion on the mechanical and biodegradable properties of an extruded Mg-1.5Zn-0.5Y-0.5Zr alloy. Materials Technology, 2022, 37, 135-142.	1.5	7
3	Effect of copper content on the biodegradation behavior of Fe-Mn-C alloy system. Materials Technology, 2022, 37, 1109-1119.	1.5	3
4	Phase formation and mechanical properties of iron-based intermetallic/steel laminate composites. Advanced Composites and Hybrid Materials, 2022, 5, 2171-2183.	9.9	7
5	Low temperature induced red-shift in violet-blue emission from Zn(Al, Ag)O nanoparticles. Materials Technology, 2022, 37, 1629-1638.	1.5	5
6	Effect of Welding Thermal Cycle on Microstructural Characteristics and Toughness in Simulated Heat Affected Zone of Low-C Medium-Mn High Strength Steel. Journal of Materials Engineering and Performance, 2022, 31, 2653-2663.	1.2	4
7	Phase reversion-induced nanostructured austenitic alloys: an overview. Materials Technology, 2022, 37, 437-449.	1.5	28
8	Developments and Perspectives on Robust Nano―and Microstructured Binderâ€Free Electrodes for Bifunctional Water Electrolysis and Beyond. Advanced Energy Materials, 2022, 12, .	10.2	63
9	Nanostructuring of biomaterials and reducing implant related infections via incorporation of silver and copper as antimicrobial elements: an overview. Materials Technology, 2022, 37, 867-879.	1.5	3
10	Enhancement of Mechanical Properties in Dissimilar Resistance Spot Welds between Galvannealed Dual Phase and Al-Si Coated Press Hardening Steels. ISIJ International, 2022, , .	0.6	0
11	Favorable Modulation of Microstructural Constituents in Governing Low Temperature Toughness Induced Through a Three-Stage Cooling Trajectory. Metals and Materials International, 2021, 27, 4152-4167.	1.8	3
12	Fabrication of biodegradable MgXCu(X=0, 0.1, 0.4, 0.7) coating on Ti6Al4V alloy with enhanced antibacterial property. Materials Technology, 2021, 36, 179-188.	1.5	7
13	TiO ₂ nanotubes synthesised on Ti-6Al-4V ELI exhibits enhanced osteogenic activity: A potential next-generation material to be used as medical implants. Materials Technology, 2021, 36, 393-399.	1.5	34
14	A Thermodynamic Analysis of Strengthening Mechanisms and Process-Structure-Property Relationships in Ti-Nb-Mo High-Strength Ferritic Alloy. Journal of Materials Engineering and Performance, 2021, 30, 2946-2954.	1.2	5
15	The Significance of Optimizing Mn-Content in Tuning the Microstructure and Mechanical Properties of δ-TRIP Steels. Metals, 2021, 11, 523.	1.0	4
16	Improvement of texture and magnetic properties of strip-cast grain-oriented electrical steel by trace Bi addition. Journal of Materials Science, 2021, 56, 11988-12000.	1.7	2
17	Recrystallization Behavior and Microstructure Evolution in Highâ€Manganese Austenitic Steel. Steel Research International, 2021, 92, 2100029.	1.0	2
18	The Significant Impact of the Characteristics of Granular Structure and Granular Bainite on the Mechanisms Contributing to Strength–Ductility Combination. Journal of Materials Engineering and Performance, 2021, 30, 7479-7487.	1.2	6

#	Article	IF	CITATIONS
19	Enhanced carbon enrichment in austenite through introducing pre-existing austenite as a â€~carbon container' in 0.2C-2Mn steel: The significant impact on microstructure and mechanical properties. Materials Characterization, 2021, 176, 111077.	1.9	6
20	The Influence of Cooling Rate on Austenite Stability and Mechanical Properties in an Austenite–Ferrite Medium-Mn Steel. Journal of Materials Engineering and Performance, 2021, 30, 7917-7925.	1.2	5
21	Austenite/ferrite interface movement during intercritical annealing of a medium Mn steel. Materials Science and Technology, 2021, 37, 745-751.	0.8	1
22	Stress and Deformation Distribution and Microstructure Changes Around Pin-Loaded Holes in Medium Manganese Steel Plates. Jom, 2021, 73, 3301-3311.	0.9	0
23	Microstructure-toughness relationship in the simulated CGHAZ of V-N microalloyed X80 pipeline steel. Materials Science and Technology, 2021, 37, 1047-1059.	0.8	4
24	Recent Advances on Development of Hydroxyapatite Coating on Biodegradable Magnesium Alloys: A Review. Materials, 2021, 14, 5550.	1.3	14
25	Ni-loss compensation and thermomechanical property recovery of 3D printed NiTi alloys by pre-coating Ni on NiTi powder. Additive Manufacturing, 2021, 47, 102344.	1.7	1
26	Effect of Zr-deoxidation on microstructure and mechanical behavior of microalloyed heavy plates with low impurity content. Journal of Iron and Steel Research International, 2021, 28, 190-200.	1.4	2
27	Additive manufacturing of dental root-analogue implant with desired properties. Materials Technology, 2021, 36, 894-906.	1.5	10
28	Precipitation Behavior of Laves Phase in the Vicinity of Oxide Film of Ferritic Stainless Steel: Selective Oxidation-Induced Precipitation. Oxidation of Metals, 2020, 93, 195-213.	1.0	15
29	Recoverable strain in a new biomedical Ti-24Nb-4Zr-8Sn alloy with cellular structure fabricated by electron beam melting. Materials Technology, 2020, 35, 881-886.	1.5	5
30	The determining role of pre-annealing on Mn partitioning behavior in medium-Mn-TRIP steel: experimental and numerical simulation. Journal of Materials Science, 2020, 55, 4437-4452.	1.7	10
31	On the electrochemical behaviour of V-N-8Cr weathering steel in simulated industrial atmosphere. Corrosion Engineering Science and Technology, 2020, 55, 159-170.	0.7	3
32	Favourable modulation of osteoblast cellular activity on Cu-containing austenitic stainless steel and comparison with the Cu-free counterpart. Materials Technology, 2020, 35, 411-420.	1.5	5
33	Commercial Scale Uniform Powder Coating for Metal Additive Manufacturing. Jom, 2020, 72, 4639-4647.	0.9	7
34	Influence of microstructure modification on corrosion resistance of friction stir processing biodegradable Mg-Zn-Nd alloy. Materials Technology, 2020, , 1-6.	1.5	3
35	Tuning austenite stability in a medium Mn steel and relationship to structure and mechanical properties. Materials Science and Technology, 2020, 36, 1308-1317.	0.8	8
36	The Impact of Isothermal Treatment on the Microstructural Evolution and the Precipitation Behavior in High Strength Linepipe Steel. Materials, 2020, 13, 634.	1.3	2

#	Article	IF	CITATIONS
37	Fatigue Failure of Gears and Bearings During Processing of Rebar Steels. Journal of Failure Analysis and Prevention, 2020, 20, 208-217.	0.5	1
38	Design of an effective heat treatment involving intercritical hardening for high-strength–high elongation of 0.2C–1.5Al–(6–8.5)Mn-Fe TRIP steels: Microstructural evolution and deformation behaviour. Materials Science and Technology, 2020, 36, 500-510.	0.8	11
39	Significant Grain Refinement in the Simulated Heat-Affected Zone (HAZ) of Ferritic Stainless Steels by Alloying with Tungsten. Metallurgical and Materials Transactions A: Physical Metallurgy and Materials Science, 2020, 51, 2719-2723.	1.1	3
40	Significant impact of cold-rolling deformation and annealing on damping capacity of Fe–Mn–Cr alloy. Journal of Iron and Steel Research International, 2020, 27, 566-576.	1.4	1
41	Effect of Ti–Mg–Ca treatment on properties of heat-affected zone after high heat input welding. Journal of Iron and Steel Research International, 2019, 26, 501-511.	1.4	16
42	Effect of Heating Rate during Continuous Annealing on Microstructure and Mechanical Properties of High-Strength Dual-Phase Steel. Journal of Materials Engineering and Performance, 2019, 28, 4556-4564.	1.2	15
43	A Novel W-Skeleton-Reinforced Al Matrix Composite by Consolidating a Newly Developed Core–Shell-Structured W-Coated Al Powder. Metallurgical and Materials Transactions A: Physical Metallurgy and Materials Science, 2019, 50, 3301-3309.	1.1	1
44	Significance of Finish Cooling Temperature to Microstructure and Property Relationship of Low-Carbon V-N-Cr Microalloyed High-Strength Steel. Journal of Materials Engineering and Performance, 2019, 28, 6492-6504.	1.2	2
45	Effect of deformation parameters in unrecrystallization range on microstructural characteristics in Al-bearing hot-rolled TRIP steel. Journal of Iron and Steel Research International, 2019, 26, 1329-1339.	1.4	1
46	Effect of prior austenite on reversed austenite stability and mechanical properties of low carbon medium manganese steel heavy plate. Materialwissenschaft Und Werkstofftechnik, 2019, 50, 1221-1231.	0.5	0
47	A General Strategy for Enhancing 3D Printability of High Laser Reflectivity Pure Aluminum Powder. Metallurgical and Materials Transactions A: Physical Metallurgy and Materials Science, 2019, 50, 4970-4976.	1.1	14
48	Relationship between high angle grain boundaries and hardness after γ→α transformation. Materials Science and Technology, 2019, 35, 1803-1814.	0.8	16
49	The Impact of Process Parameters on Microstructure and Mechanical Properties of Stainless Steel/Carbon Steel Clad Rebar. Materials, 2019, 12, 2868.	1.3	10
50	Interaction Between Natural Aging and Pre-Aging Processes and its Impact on the Age-Hardening Behavior of Al-Mg-Si Automotive Sheets. Jom, 2019, 71, 4405-4413.	0.9	3
51	Softening and recrystallization behavior of a new class of ferritic steel. Journal of Iron and Steel Research International, 2019, 26, 154-161.	1.4	2
52	Bioactive coating on a new Mg-2Zn-0.5Nd alloy: modulation of degradation rate and cellular response. Materials Technology, 2019, 34, 394-402.	1.5	13
53	A medium-Mn steel processed by novel twin-roll strip casting route. Materials Science and Technology, 2019, 35, 1227-1238.	0.8	10
54	Influence of Inter-Pass Cooling on Microstructural Evolution and Plastic Deformation of Heavy EH47 Plates. Materials, 2019, 12, 1686.	1.3	1

#	Article	IF	CITATIONS
55	Activating Trace Fe Impurity as Catalyst to Plant Carbon Nanotubes Within Ti-6Al-4V Powders for High-Performance Ti Metal Matrix Composites. Metallurgical and Materials Transactions A: Physical Metallurgy and Materials Science, 2019, 50, 3975-3979.	1.1	6
56	Fracture toughness behavior of low-C medium-Mn high-strength steel with submicron-scale laminated microstructure of tempered martensite and reversed austenite. Journal of Materials Science, 2019, 54, 12095-12105.	1.7	14
57	Correlation between microstructure and impact toughness of weld heat-affected zone in 5Âwt.% manganese steels. Journal of Iron and Steel Research International, 2019, 26, 761-770.	1.4	2
58	Effect of Ca on microstructure and high temperature creep properties of AM60-1Ce alloy. China Foundry, 2019, 16, 88-96.	0.5	3
59	Effect of Tempering Mode on the Microstructure and Mechanical Properties of a Lean Alloy Martensitic Steel: Conventional Reheating Versus Induction Reheating. Journal of Materials Engineering and Performance, 2019, 28, 2807-2815.	1.2	3
60	On the Optimization of Microstructure and Mechanical Properties of CrWMn Tool Steel by Deep Cryogenic Treatment. Steel Research International, 2019, 90, 1800523.	1.0	5
61	First principles calculation of interfacial stability, energy, and elemental diffusional stability of Fe (111)/Al2O3 (0001) interface. AlP Advances, 2019, 9, .	0.6	12
62	The Significant Impact of Carbon Nanotubes on the Electrochemical Reactivity of Mg-Bearing Metallic Glasses with High Compressive Strength. Materials, 2019, 12, 2989.	1.3	5
63	Variation in Morphology and Kinetics of Granular Bainite with Welding Thermal Cycles in High-Nb Fire-Resistant Steel: Experiments and Theoretical Calculations. Journal of Materials Engineering and Performance, 2019, 28, 321-329.	1.2	2
64	Corrosion Behavior of High-Strength Steel for Flexible Riser Exposed to CO2-Saturated Saline Solution and CO2-Saturated Vapor Environments. Acta Metallurgica Sinica (English Letters), 2019, 32, 607-617.	1.5	12
65	A comparative study on the tribological behavior of Ti-6Al-4V and Ti-24Nb-4Zr-8Sn alloys in simulated body fluid. Materials Technology, 2019, 34, 270-284.	1.5	17
66	High strength and ductility combination in nano-/ultrafine-grained medium-Mn steel by tuning the stability of reverted austenite involving intercritical annealing. Journal of Materials Science, 2019, 54, 6565-6578.	1.7	85
67	Effect of Cooling Rates in Coiling Process on Microstructures and Mechanical Properties in Al-Bearing Hot-Rolled TRIP Steel. Acta Metallurgica Sinica (English Letters), 2019, 32, 1207-1218.	1.5	4
68	On the influence of deformation mechanism during cold and warm rolling on annealing behavior of a 304 stainless steel. Materials Science & Engineering A: Structural Materials: Properties, Microstructure and Processing, 2019, 746, 341-355.	2.6	78
69	Retained austenite stabilisation in low carbon high silicon steel during isothermal holding. Materials Science and Technology, 2019, 35, 45-54.	0.8	6
70	Strain rate dependence on the evolution of microstructure and deformation mechanism during nanoscale deformation in low carbon-high Mn TWIP steel. Materials Science & Engineering A: Structural Materials: Properties, Microstructure and Processing, 2019, 742, 116-123.	2.6	28
71	Combined contribution of Cu-rich precipitates and retained austenite on mechanical properties of a novel low-carbon medium-Mn steel plate. Journal of Materials Science, 2019, 54, 3438-3454.	1.7	17
72	Aging phenomenon in low lattice-misfit cobalt-free maraging steel: Microstructural evolution and strengthening behavior. Materials Science & Engineering A: Structural Materials: Properties, Microstructure and Processing, 2019, 739, 445-454.	2.6	37

#	Article	IF	CITATIONS
73	Hot Deformation Behavior and Processing Maps of a Medium Manganese TRIP Steel. Acta Metallurgica Sinica (English Letters), 2019, 32, 1021-1031.	1.5	15
74	Nanomaterials in microfluidics for disease diagnosis and therapy development. Materials Technology, 2019, 34, 92-116.	1.5	22
75	Innovative processing of obtaining nanostructured bainite with high strength - high ductility combination in low-carbon-medium-Mn steel: Process-structure-property relationship. Materials Science & Engineering A: Structural Materials: Properties, Microstructure and Processing, 2018, 718. 267-276.	2.6	42
76	Microstructural Evolution and the Precipitation Behavior in X90 Linepipe Steel During Isothermal Processing. Journal of Materials Engineering and Performance, 2018, 27, 1494-1504.	1.2	6
77	Surface biodegradation behavior of rare earth- containing magnesium alloys with different microstructure: the impact on apatite coating formation on the surface. Materials Technology, 2018, 33, 488-494.	1.5	10
78	The significance and design of hybrid process in governing high strength-high toughness combination of fiber laser-welded T-250 maraging steel joint. Materials Science & Engineering A: Structural Materials: Properties, Microstructure and Processing, 2018, 718, 173-181.	2.6	5
79	Effect of vacuum level on microstructure and mechanical properties of titanium–steel vacuum roll clad plates. Journal of Iron and Steel Research International, 2018, 25, 72-80.	1.4	23
80	Selective role of bainitic lath boundary in influencing slip systems and consequent deformation mechanisms and delamination in high-strength low-alloy steel. Philosophical Magazine, 2018, 98, 934-958.	0.7	7
81	Evolution of microstructure and tensile properties during the three-stage heat treatment of TA19 titanium alloy. Materials Science & Engineering A: Structural Materials: Properties, Microstructure and Processing, 2018, 716, 157-164.	2.6	42
82	Ensuring combination of strength, ductility and toughness in medium-manganese steel through optimization of nano-scale metastable austenite. Materials Characterization, 2018, 136, 20-28.	1.9	131
83	Surface nanotopography-induced favorable modulation of bioactivity and osteoconductive potential of anodized 3D printed Ti-6Al-4V alloy mesh structure. Journal of Biomaterials Applications, 2018, 32, 1032-1048.	1.2	46
84	Strengthening of cobalt-free 19Ni3Mo1.5Ti maraging steel through high-density and low lattice misfit nanoscale precipitates. Materials Science & Engineering A: Structural Materials: Properties, Microstructure and Processing, 2018, 715, 174-185.	2.6	47
85	Effect of rolling temperature on the microstructure, texture, and magnetic properties of strip-cast grain-oriented 3% Si steel. Journal of Materials Science, 2018, 53, 9217-9231.	1.7	7
86	The significance of macromolecular architecture in governing structure-property relationship for biomaterial applications: an overview. Materials Technology, 2018, 33, 364-386.	1.5	18
87	High-cycle fatigue behavior of low-C medium-Mn high strength steel with austenite-martensite submicron-sized lath-like structure. Materials Science & Engineering A: Structural Materials: Properties, Microstructure and Processing, 2018, 718, 477-482.	2.6	35
88	Ultra-high cycle fatigue property of a multiphase steel microalloyed with niobium. Materials Science & Engineering A: Structural Materials: Properties, Microstructure and Processing, 2018, 718, 1-8.	2.6	13
89	Design of novel Fe–Mn–Ni cryogenic steel: microstructure-property relationship during simulated welding. Science and Technology of Welding and Joining, 2018, 23, 125-133.	1.5	2
90	Influence of intercritical tempering temperature on impact toughness of a quenched and tempered medium-Mn steel: Intercritical tempering versus traditional tempering. Materials Science & Engineering A: Structural Materials: Properties, Microstructure and Processing, 2018, 711, 484-491.	2.6	38

#	Article	IF	CITATIONS
91	On the strain rate sensitivity of aluminum-containing transformation-induced plasticity steels: Interplay between TRIP and TWIP effects. Materials Science & Engineering A: Structural Materials: Properties, Microstructure and Processing, 2018, 711, 515-523.	2.6	19
92	The contribution of long-period stacking-ordered structure (LPSO) to high strength-high ductility combination and nanoscale deformation behavior of magnesium-rare earth alloy. Materials Science & amp; Engineering A: Structural Materials: Properties, Microstructure and Processing, 2018, 713, 112-117.	2.6	38
93	Effect of inorganic nanofillers on the impact behavior and fracture probability of industrial high-density polyethylene nanocomposite. Journal of Composite Materials, 2018, 52, 2431-2442.	1.2	10
94	Microstructure and magnetic properties of strip-cast grain-oriented 4.5%Si steel under isochronal and isothermal secondary annealing. Journal of Materials Science, 2018, 53, 2928-2941.	1.7	8
95	Hot Deformation Behavior and Processing Maps of a High Al-low Si Transformation-Induced Plasticity Steel: Microstructural Evolution and Flow Stress Behavior. Acta Metallurgica Sinica (English) Tj ETQq1 1 0.784314	ngങT /Ove	er lø ck 10 Tf
96	Design and biological functionality of a novel hybrid Tiâ€6 <scp>A</scp> lâ€4 <scp>V</scp> /hydrogel system for reconstruction of bone defects. Journal of Tissue Engineering and Regenerative Medicine, 2018, 12, 1133-1144.	1.3	33
97	Structure–property relationships in heat-affected zone of gas-shielded arc-welded V–N microalloyed steel. Journal of Iron and Steel Research International, 2018, 25, 1244-1254.	1.4	5
98	The Determining Role of Nb Interlayer on Interfacial Microstructure and Mechanical Properties of Ti/Steel Clad Plate by Vacuum Rolling Cladding. Materials, 2018, 11, 1983.	1.3	16
99	The Impact of Surface Treatment and Degree of Vacuum on the Interface and Mechanical Properties of Stainless Steel Clad Plate. Materials, 2018, 11, 1489.	1.3	14
100	Effect of thermal treatment on the evolution of delta ferrite in 11Cr–3Co–2.3W steel. Materials Science and Technology, 2018, 34, 2087-2096.	0.8	10
101	On the origin and contribution of extended kinks and jogs and stacking fault ribbons to deformation behavior in an ultrahigh strength cobalt-free maraging steel with high density of low lattice misfit precipitates. Materials Science & amp; Engineering A: Structural Materials: Properties, Microstructure and Processing, 2018, 728, 208-217.	2.6	14
102	Effect of interfacial compounds on mechanical properties of titanium–steel vacuum roll-cladding plates. Materials Science and Technology, 2018, 34, 1700-1709.	0.8	19
103	The significance of deformation mechanisms on the fracture behavior of phase reversion-induced nanostructured austenitic stainless steel. Scientific Reports, 2018, 8, 7908.	1.6	14
104	Effect of Tempered Martensite and Ferrite/Bainite on Corrosion Behavior of Low Alloy Steel Used for Flexible Pipe Exposed to High-Temperature Brine Environment. Journal of Materials Engineering and Performance, 2018, 27, 4911-4920.	1.2	18
105	Alginate/poly(amidoamine) injectable hybrid hydrogel for cell delivery. Journal of Biomaterials Applications, 2018, 33, 295-314.	1.2	12
106	Microstructure and mechanical properties of a novel hot-rolled 4% Mn steel processed by intercritical annealing. Journal of Materials Science, 2018, 53, 12570-12582.	1.7	11
107	Cellular response of <i>Staphylococcus aureus </i> to nanostructured metallic biomedical devices: surface binding and mechanism of disruption of colonization. Materials Technology, 2017, 32, 22-31.	1.5	48
108	Extending the boundaries of mechanical properties of Ti-Nb low-carbon steel via combination of ultrafast cooling and deformation during austenite-to-ferrite transformation. Metals and Materials International, 2017, 23, 175-183.	1.8	19

#	Article	IF	CITATIONS
109	Effect of two-step intercritical annealing on microstructure and mechanical properties of hot-rolled medium manganese TRIP steel containing δferrite. Materials Science & Engineering A: Structural Materials: Properties, Microstructure and Processing, 2017, 688, 40-55.	2.6	63
110	Corrosion Behavior of Low-Alloy Pipeline Steel Exposed to H2S/CO2-Saturated Saline Solution. Journal of Materials Engineering and Performance, 2017, 26, 1010-1017.	1.2	14
111	Biodegradable hydrogelâ€based biomaterials with high absorbent properties for nonâ€adherent wound dressing. International Wound Journal, 2017, 14, 1076-1087.	1.3	46
112	Atom probe tomography and numerical study of austenite stabilization in a low carbon low alloy steel processed by two-step intercritical heat treatment. Scripta Materialia, 2017, 137, 36-40.	2.6	27
113	Correlation between deformation behavior and austenite characteristics in a Mn-Al type TRIP steel. Materials Science & Engineering A: Structural Materials: Properties, Microstructure and Processing, 2017, 698, 126-135.	2.6	43
114	Effect of deep cryogenic treatment on structure-property relationship in an ultrahigh strength Mn-Si-Cr bainite/martensite multiphase rail steel. Materials Science & Engineering A: Structural Materials: Properties, Microstructure and Processing, 2017, 684, 559-566.	2.6	30
115	Evolution of microstructure and crystallographic texture of microalloyed steel during warm rolling in dual phase region and their influence on mechanical properties. Materials Science & Engineering A: Structural Materials: Properties, Microstructure and Processing, 2017, 685, 194-204.	2.6	36
116	Significant influence of carbon and niobium on the precipitation behavior and microstructural evolution and their consequent impact on mechanical properties in microalloyed steels. Materials Science & amp; Engineering A: Structural Materials: Properties, Microstructure and Processing, 2017, 683, 70-82.	2.6	20
117	Effect of interpass temperature on the microstructure and mechanical properties of multi-pass weld metal in a 550-MPa-grade offshore engineering steel. Welding in the World, Le Soudage Dans Le Monde, 2017, 61, 1155-1168.	1.3	41
118	Nanoscale spheroidized cementite induced ultrahigh strength-ductility combination in innovatively processed ultrafine-grained low alloy medium-carbon steel. Scientific Reports, 2017, 7, 2679.	1.6	32
119	Tunable TiO2–pepsin thin film as a low-temperature electron transport layer for photoelectrochemical cells. Materials Technology, 2017, 32, 829-837.	1.5	18
120	The role of Cu and Al addition on the microstructure and fracture characteristics in the simulated coarse-grained heat-affected zone of high-strength low-alloy steels with superior toughness. Materials Science and Technology, 2017, 33, 1750-1764.	0.8	13
121	Comparison of corrosion behaviors of lowâ€alloy steel exposed to vaporâ€saturated H ₂ S/CO ₂ and H ₂ S/CO ₂ â€saturated brine environments. Materials and Corrosion - Werkstoffe Und Korrosion, 2017, 68, 566-579.	0.8	8
122	Precipitation of carbonitrides and high-temperature strength in heat-affected zone of high-Nb containing fire-resistant steel. Science and Technology of Welding and Joining, 2017, 22, 157-165.	1.5	6
123	<scp>C</scp> ellular response of osteoblasts to low modulus Tiâ€24Nbâ€4Zrâ€8Sn alloy mesh structure. Journal of Biomedical Materials Research - Part A, 2017, 105, 859-870.	2.1	50
124	Interplay between reversed austenite and plastic deformation in a directly quenched and intercritically annealed 0.04C-5Mn low-Al steel. Journal of Alloys and Compounds, 2017, 695, 2072-2082.	2.8	39
125	Understanding the response of pulsed electric field on osteoblast functions in three-dimensional mesh structures. Journal of Biomaterials Applications, 2016, 31, 594-605.	1.2	19
126	Biological functionality and mechanistic contribution of extracellular matrixâ€ornamented three dimensional Tiâ€6Alâ€4V mesh scaffolds. Journal of Biomedical Materials Research - Part A, 2016, 104, 2751-2763.	2.1	37

#	Article	IF	CITATIONS
127	Biological functionality of extracellular matrixâ€ornamented threeâ€dimensional printed hydroxyapatite scaffolds. Journal of Biomedical Materials Research - Part A, 2016, 104, 1343-1351.	2.1	60
128	Cellular response ofEscherichia colito Mg-2Zn-2Gd alloy with different grain structure: mechanism of disruption of colonisation. Materials Technology, 2016, 31, 836-844.	1.5	28
129	Effect of microstructure on the crack propagation behavior of microalloyed 560MPa (X80) strip during ultra-fast cooling. Materials Science & Engineering A: Structural Materials: Properties, Microstructure and Processing, 2016, 666, 214-224.	2.6	48
130	Ultrahigh strength-toughness combination in Bainitic rail steel: The determining role of austenite stability during tempering. Materials Science & Engineering A: Structural Materials: Properties, Microstructure and Processing, 2016, 662, 162-168.	2.6	70
131	Microstructure-property relationship in bainitic steel: The effect of austempering. Materials Science & Engineering A: Structural Materials: Properties, Microstructure and Processing, 2016, 675, 120-127.	2.6	35
132	Biomimetic nanostructured hydroxyapatite coatings on metallic implant materials. Materials Technology, 2016, 31, 782-790.	1.5	34
133	Biological activity of nanostructured metallic materials for biomedical applications. Materials Technology, 2016, 31, 772-781.	1.5	17
134	The effect of warm deforming and reversal austenization on the microstructure and mechanical properties of a microalloyed steel. Materials Science & Engineering A: Structural Materials: Properties, Microstructure and Processing, 2016, 671, 182-189.	2.6	8
135	A Novel thermo-mechanical controlled processing for large-thickness microalloyed 560 MPa (X80) pipeline strip under ultra-fast cooling. Materials Science & Engineering A: Structural Materials: Properties, Microstructure and Processing, 2016, 673, 373-377.	2.6	11
136	High performance bifunctional electrocatalytic activity of a reduced graphene oxide–molybdenum oxide hybrid catalyst. Journal of Materials Chemistry A, 2016, 4, 13271-13279.	5.2	62
137	Austenite stability and its effect on the toughness of a high strength ultra-low carbon medium manganese steel plate. Materials Science & Engineering A: Structural Materials: Properties, Microstructure and Processing, 2016, 675, 153-163.	2.6	127
138	Degradation behaviour of magnesium-rare earth biomedical alloys. Materials Technology, 2016, 31, 726-731.	1.5	41
139	Processing-structure-mechanical property relationship in Ti-Nb microalloyed steel: Continuous cooling versus interrupted cooling. Materials Science & Engineering A: Structural Materials: Properties, Microstructure and Processing, 2016, 671, 254-263.	2.6	16
140	Nanoscale precipitates strengthened lanthanum-bearing Mg-3Sn-1Mn alloys through continuous rheo-rolling. Scientific Reports, 2016, 6, 23154.	1.6	35
141	Microstructure and Mechanism of Strengthening of Microalloyed Pipeline Steel: Ultra-Fast Cooling (UFC) Versus Laminar Cooling (LC). Journal of Materials Engineering and Performance, 2016, 25, 2511-2520.	1.2	9
142	Phase reverted transformation-induced nanograined microalloyed steel: Low temperature superplasticity and fracture. Materials Science & Engineering A: Structural Materials: Properties, Microstructure and Processing, 2016, 668, 105-111.	2.6	17
143	Interplay between selfâ€assembled structure of bone morphogenetic proteinâ€2 (<scp>BMP</scp> â€2) and osteoblast functions in threeâ€dimensional titanium alloy scaffolds: <scp>S</scp> timulation of osteogenic activity. Journal of Biomedical Materials Research - Part A, 2016, 104, 517-532.	2.1	57
144	The functional response of bioactive titaniaâ€modified threeâ€dimensional Tiâ€6Alâ€4V mesh structure toward providing a favorable pathway for intercellular communication and osteoincorporation. Journal of Biomedical Materials Research - Part A, 2016, 104, 2488-2501.	2.1	27

#	Article	IF	CITATIONS
145	Determination of the mechanical, thermal and physical properties of nano-CaCO ₃ filled high-density polyethylene nanocomposites produced in an industrial scale. Journal of Composite Materials, 2016, 50, 3445-3456.	1.2	22
146	Chitosan-gelatin-based microgel for sustained drug delivery. Journal of Biomaterials Science, Polymer Edition, 2016, 27, 441-453.	1.9	54
147	Epsilon carbide precipitation and wear behaviour of low alloy wear resistant steels. Materials Science and Technology, 2016, 32, 320-327.	0.8	49
148	The influence of cell morphology on the compressive fatigue behavior of Ti-6Al-4V meshes fabricated by electron beam melting. Journal of the Mechanical Behavior of Biomedical Materials, 2016, 59, 251-264.	1.5	194
149	Mechanistic contribution of electroconductive hydroxyapatite–titanium disilicide composite on the alignment and proliferation of cells. Journal of Biomaterials Applications, 2016, 30, 1505-1516.	1.2	15
150	Investigation of mechanical, thermal and surface properties of nanoclay/HDPE nanocomposites produced industrially by melt mixing approach. Journal of Composite Materials, 2016, 50, 3105-3116.	1.2	37
151	Electric field-mediated growth of osteoblasts – the significant impact of dynamic flow of medium. Biomaterials Science, 2016, 4, 136-144.	2.6	28
152	Structure–mechanical property relationship in a low-C medium-Mn ultrahigh strength heavy plate steel with austenite-martensite submicro-laminate structure. Materials Science & Engineering A: Structural Materials: Properties, Microstructure and Processing, 2015, 647, 144-151.	2.6	57
153	Characterization of Microstructure and Texture in Grain-Oriented High Silicon Steel by Strip Casting. Acta Metallurgica Sinica (English Letters), 2015, 28, 1394-1402.	1.5	11
154	Austenite stability and deformation behavior in a cold-rolled transformation-induced plasticity steel with medium manganese content. Acta Materialia, 2015, 84, 229-236.	3.8	343
155	Structure–mechanical property relationship in a high strength low carbon alloy steel processed by two-step intercritical annealing and intercritical tempering. Materials Science & Engineering A: Structural Materials: Properties, Microstructure and Processing, 2014, 607, 569-577.	2.6	40
156	On the Microstructure and Wear Behavior of Feâ€Based/B 4 C Composite Coating Processed by Vacuum Cladding. Steel Research International, 0, , 2100400.	1.0	0
157	Dynamic Deformation of Low-Alloyed Transformation-Induced Plasticity-Aided Steel from Low to High Strain Rates. Journal of Materials Engineering and Performance, 0, , 1.	1.2	0